Solid Oxide Membrane (SOM)-Based Technology for Carbon-Free Efficient Production of Solar-Grade Silicon

Haoxuan Yan, Michelle Sugimoto, Adam Powell, and Uday Pal

Abstract State-of-the-art solar-grade silicon production is energy intensive and has a negative impact on the environment. Due to the robust and rapid growth of the Si-based photovoltaic (PV) industry, it is necessary to develop a greener technology for silicon production. Solid oxide membrane (SOM) electrolysis is a proven versatile green technology that can be developed to economically produce many important metal or metal compounds from their oxides. This work will discuss application of SOM electrolysis to produce solar-grade silicon from silica in a single-step resulting in net-zero-carbon emission. The high-temperature SOM electrolysis cell employs stable molten oxide-fluoride bath with silicon wafer cathode and stabilized zirconia membrane-based novel anodes. The cell design and process parameters are selected to enable silicon deposition on the Si wafer cathode. However, initially an electrochemical oxidation reaction occurred between silicon and oxygen that involved the cathode/flux/gas interfaces. An approach to successfully prevent this side reaction has been demonstrated. Electrochemical characterization of the SOM process is presented, and post-experimental characterization demonstrates Si deposits in the form of silicon carbide due to the use of graphite crucible and graphite current collector.

H. Yan · U. Pal (✉)
Division of Materials Science and Engineering, Boston University, 15 St Mary's St, Boston, MA, USA
e-mail: upal@bu.edu

H. Yan
e-mail: hyan910@bu.edu

M. Sugimoto · U. Pal
Department of Mechanical Engineering, Boston University, 110 Cummington Mall, Boston, MA, USA
e-mail: msugi@bu.edu

A. Powell
Department of Mechanical Engineering, Worcester Polytechnic Institute, 100 Institute Rd, Worcester, MA 01609, USA
e-mail: acpowell@wpi.edu

A. Lazou et al. (eds.), *REWAS 2022: Developing Tomorrow's Technical Cycles (Volume I)*, The Minerals, Metals & Materials Series,
https://doi.org/10.1007/978-3-030-92563-5_69

Keywords SOM electrolysis · Silicon production · Green technology

Introduction

Currently, industrial processes that produce silicon rely on multi-step batch units which are energy intensive, capital intensive, and environmentally unsound due to the heavy emission of pollutants and greenhouse gases [1, 2]. An innovative technology, solid oxide membrane (SOM) electrolysis, has been developed and successfully applied in extraction of metals or alloys from their oxides. Previous research that incorporated this technology has proven its feasibility producing a variety of metals including tantalum, titanium, ytterbium, magnesium, and aluminum [3–8]. In contrast to conventional silicon production methods, such as the Siemens process and fluidized bed reactors, the SOM technology has three main advantages: it is a single-step batch operation that is less energy and capital intensive, it does not release any direct greenhouse gases or halogenated emissions, and it yields pure O_2 as a valuable by-product [9]. It does so by efficiently electrolyzing silica in a well-engineered flux, the silicon is deposited at the cathode and the oxygen ions migrate through a ceramic solid oxygen ion conducting stabilized zirconia membrane to the anode where O_2 gas is evolved.

Three key innovations are needed for the successful operation of the SOM electrolytic cell: (i) the YSZ membrane needs to separate the anode from the flux. This prevents the oxygen gas produced at the anode from contacting the reduced metal at the cathode; (ii) a flux needs to be engineered that has high ionic conductivity, low electronic conductivity, low volatility, and high chemical stability in contact with the YSZ membrane; and (iii) a cathode current collector needs to be developed that is thermally and chemically stable in the SOM environment, has low resistance while contacting the silicon wafer cathode. This allows the cathode to be removed from the flux after the experiment. The first two innovations have been successfully implemented while developing a suitable cathode current collector still remains a challenge.

In this work, graphite is chosen as the cathode current collector because it has adequate electrical conductivity at high temperature, high chemical stability in contact with the flux, good machinability that enables secure connection and contact with the Si wafer cathode. The design details are described in the experimental section. For the ease of operation and to demonstrate process feasibility, graphite is also employed as the anode current collector with liquid silver serving as the anode. In this case the oxygen produced at the anode reacts with the carbon to form carbon monoxide (CO). Initially, an electrochemical oxidation reaction involving the silicon wafer, flux, graphite, and impurity oxygen in the gas phase consumed the silicon wafer cathode. The oxidation mechanism was identified and later mitigated by immersing the silicon wafer deeper into the flux. The SOM electrolysis deposited silicon which reacted with the carbon to form silicon carbide as predicted by the

Si-C-O phase stability diagram. Future work regarding stabilizing the pure Si phase free of carbon in the system is proposed.

Experimental Work

A proof-of-concept laboratory scale Si-SOM electrolysis was performed using the setup shown in Fig. 1. The setup consists of a graphite crucible that was heated to 1100 °C in forming gas (95% Argon–5%H2) to ensure an inert atmosphere. Inside the crucible, 450 g of powdered flux (45wt% MgF_2–55wt% CaF_2 with 5wt% SiO_2, 9wt% CaO, and 4wt% YF_3, suggested and verified by previous studies) was used to form the molten salt electrolyte [10–15]. All fluorides and oxides were pre-baked before melting, and salt flux without SiO_2 was pre-melted to prevent the formation of SiF_4(g). A one end-closed 8 mol% Yttria-stabilized zirconia (YSZ) membrane tube separated the flux from 5 g of liquid silver enclosed inside the YSZ tube. An alumina tube was used to attach YSZ membrane with gas-sealing ceramic paste (Aremco 552) for extra length. A graphite anode current collector was placed in the YSZ membrane tube and submerged in the liquid silver at the target temperature. A graphite rod is used as the current collector. A slit is machined at the end of the graphite rod and the silicon wafer is inserted and glued using graphite paste (Resbond 931). Two tungsten reference electrodes were inserted in the molten flux to monitor the electrochemical behavior of the flux during the electrolysis. The reference electrodes were electrically insulated by alumina tubes. A stainless-steel bubbling tube was submerged into the flux during the electrolysis to ensure that the molten flux is homogeneous and to reduce concentration polarization near the Si wafer cathode. The entire cell was operated in a vertical tube furnace with the cell placed in the center of the hot zone.

Si Wafer Stability Analysis—It was noted earlier that the Si wafer cathode experienced some oxidation or thinning when the Si wafer was removed from the flux after some initial SOM electrolysis experiments. Following this observation, a series of silicon wafer stability tests were performed. The graphite current collector with the silicon wafer cathode were heated to 1100 C in the reducing environment (95% Argon–5%H2) and immersed into the flux at different depths for 6 h. The flow rate

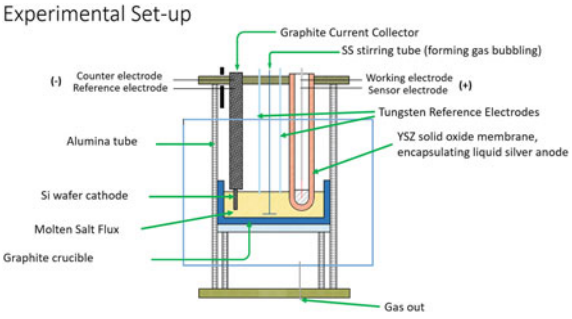

Fig. 1 Schematics of the SOM cell

of the forming gas was fixed at 50 ccm. In one of the tests the cathode current collector with the silicon wafer was placed above the flux for the same length of time (6 h) to evaluate the effect of trace amounts of oxygen in the system on the oxidation behavior of the silicon wafer. After these experiments, the silicon wafer was removed, sectioned, and mounted in epoxy to examine the microstructure under Zeiss Supra 55 scanning electron microscope equipped with EDAX EDS analyzer.

Electrochemical Measurements—Several electrochemical measurements were performed during the electrolysis. To monitor the behavior of the flux, the two tungsten rods were inserted into the flux periodically and electrochemical impedance spectroscopy (EIS) measurements were made. The current is also measured with small applied Potentiostatic hold below the dissociation potentials of oxides in the flux. These measurements were carried out with a Princeton Applied Research 263A Potentiostat and a Solartron 1250 frequency response analyzer. From these measurements the ionic and electronic transference numbers in the flux were determined. Also, prior to performing the SOM electrolysis, a potentiodynamic scan was performed across the anode and the cathode to determine the dissociation potential of silicon oxide and possibly other impurity oxides in the flux. The overall cell resistance was estimated from the linear portion of this scan. After these measurements were made, SOM electrolysis was performed above the dissociation potential of silica (0.95 V) for 8 h. Current versus time was recorded with a Princeton Applied Research 263A Potentiostat, and the gas bubbling from the anode inside the YSZ tube was also recorded using a digital mass flowmeter. After 8 h, when the electrolysis was complete, the anode was removed while the cathode remained inside the flux. Finally, the two tungsten reference electrodes were once again inserted into the flux to determine if there were any changes in the electrochemical behavior of the flux because of the electrolysis process. All electrochemical measurements were made at 1100 C under a forming gas (95% Argon–5%H2) flow rate of 50 ccm.

Post SOM electrolysis Characterization—After the experiment, the furnace is allowed to cool and the cathode with the solidified flux is removed and sectioned. The sectioned piece is mounted in epoxy and examined under the Zeiss Supra 55 scanning electron microscope (SEM) with the EDAX EDS system. A portion of the YSZ tube that contains the silver anode was also cross-sectioned and examined with the same instrument. The objective of the post characterization work is to determine the nature of the silicon deposition and ensure that the YSZ membrane was stable in contact with the flux.

Results and Discussion

Si Wafer Stability Analysis—As-received silicon wafer was sectioned and mounted without heating in the reducing environment to evaluate its thickness. The SEM/EDS examination showed the thickness to be 507 μm with no observable layer of silicon oxide (Fig. 2a). To determine the effect of the experimental gas environment in the reactor, the silicon wafer was heated to 1100 C in forming gas. It was found that

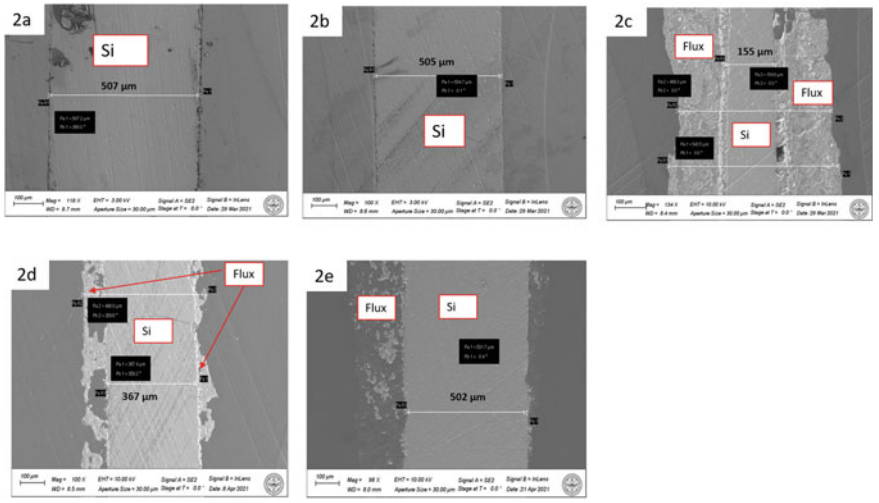

Fig. 2 SEM images of silicon wafer **a** as received, **b** above the flux at 1100 C for 6 h, **c** partially immersed in flux at 1100 C for 6 h, **d** completely immersed at 1.5 cm deep in the flux at 1100 C for 6 h, **e** completely immersed at 3 cm deep in the flux at 1100 C for 6 h

the thickness of the silicon wafer decreased by 4 µm and a very thin layer of silicon oxide formed on the surface (Fig. 2b). Next the silicon wafer was partially immersed in the flux. A significant amount of thinning was observed in the portion of the silicon wafer that was immersed in the flux. This portion of the wafer was only 155 µm thick (Fig. 2c). In subsequent experiments the silicon wafers were completely immersed in the flux to a depth of 1.5 cm and 3 cm, respectively. The silicon wafer that was 1.5 cm deep had a final thickness of 367 µm while the one that was 3 cm deep had a thickness of 503 µm. This indicates that the thinning of the wafer decreases with immersion depth in the flux.

Silicon wafer thinning mechanism—Fig. 2b suggests that the oxygen impurity in the forming gas environment reacts to form a very thin protective oxide scale that is only 3 µm thick on a silicon wafer that is originally 507 µm thick. However, when the silicon wafer is immersed in the flux the thinning continues and it is dependent on the immersion depth of the wafer. This mechanism is shown in Fig. 3. At the flux/gas interface the impurity oxygen in the gas phase is reduced in the presence of an electronic conductor (graphite or silicon) to oxygen ions. The silicon wafer is oxidized at the wafer/flux interface to silicon ions. Thus, the silicon wafer oxidation reaction is aided by the ionic flux while the rate of the reaction is controlled by the electron and the oxygen ion transfer between the oxidation and the reduction reaction sites. Hence it was seen that as the resistance to electron-oxygen ion transfer is increased by increasing the immersion depth. The rate of the silicon thinning also decreased.

To prevent silicon wafer thinning during SOM electrolysis, the immersion depth of the silicon wafer was always maintained at 4.5 cm from the flux/gas interface.

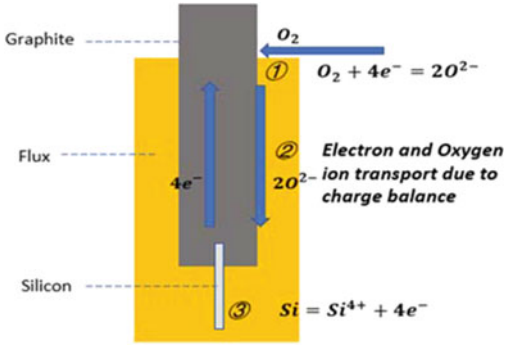

Fig. 3 Reaction mechanism of silicon wafer thinning

Electrochemical Measurements—The impedance measured between the two reference electrodes Fig. 4a provides the total salt resistance while the current measured between the electrodes at very low applied potentials (below the dissociation potentials of the oxides) provides the electronic resistance. From these two measured resistance values, it is possible to determine the ionic and electronic transference numbers [16]. Measurements made before and after electrolysis show that the flux remains primarily ionic throughout the experiment (see Table 1).

The potentiodynamic scan between the anode and the cathode confirms a dissociation potential of 0.51 V (Fig. 4a) corresponding to the following overall cell reaction: $SiO_2 + 2C = Si + 2CO(g)$ at 1100 C. From the linear portion of the current–potential scan the overall cell resistance was estimated to be around 0.5 Ω. In comparison with previous SOM cells, it appears that this cell also has low overall resistance, low electronic and high ionic conductivities, and is able to effectively dissociate SiO_2 [6, 7, 13].

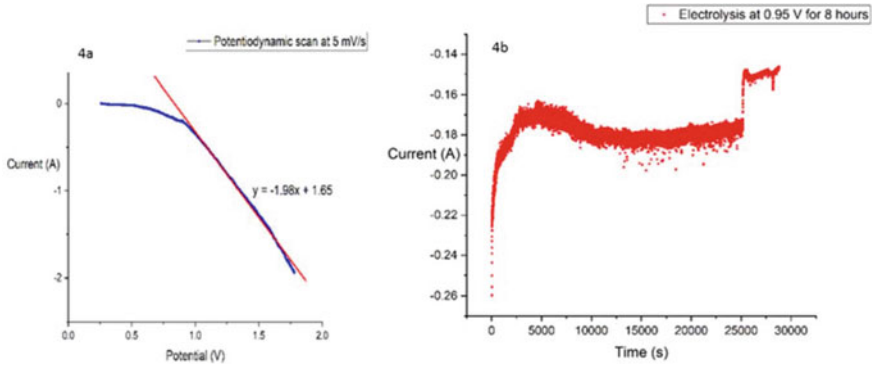

Fig. 4 Electrochemical measurements **a** Potentiodynamic scan at 5 mV/s across cathode and anode **b** Current–time curve during the electrolysis under an applied potential of 0.95 V for 8 h

Table 1 Electronic and ionic transferences number of the salt (flux) before and after the electrolysis

	Total resistance (Ω)	Electronic resistance (Ω)	Electronic transference number, t_e	Ionic transference number, t_i
Before electrolysis	0.11	42.144	2.6e-3	0.99740
After electrolysis	0.17	294.612	5.7e-4	0.99943

Figure 4b shows the electrolysis current with 0.95 V applied potential between the electrodes. During 8 h of electrolysis the current–time plot was stable. The measured changes in current and the recorded anodic gas evolution corresponded well with each other. The anodic gas bubbling was measured to be 4.1 ccm during the first 25,000 s and 3.7 ccm for the remainder of the time, in line with the small observed drop in the current drop from 0.17 to 0.14 A at the 25,000 s mark. The reason for this small drop in the current is not clear. Taking the integral of the current–time curve, 0.36 g of silicon should have been produced under Faradaic conditions which corresponds to a 3 mm thick planar deposit.

Post SOM electrolysis Characterization—The SEM images of sectioned silicon wafer are shown in Fig. 5a–c. Figure 5a shows the EDS mapping of the silicon/flux interface. It was observed that 20 μm thick silicon carbide deposited on the Si wafer cathode (Fig. 5b) instead of 3 mm as predicted based on Faradaic conversion of the

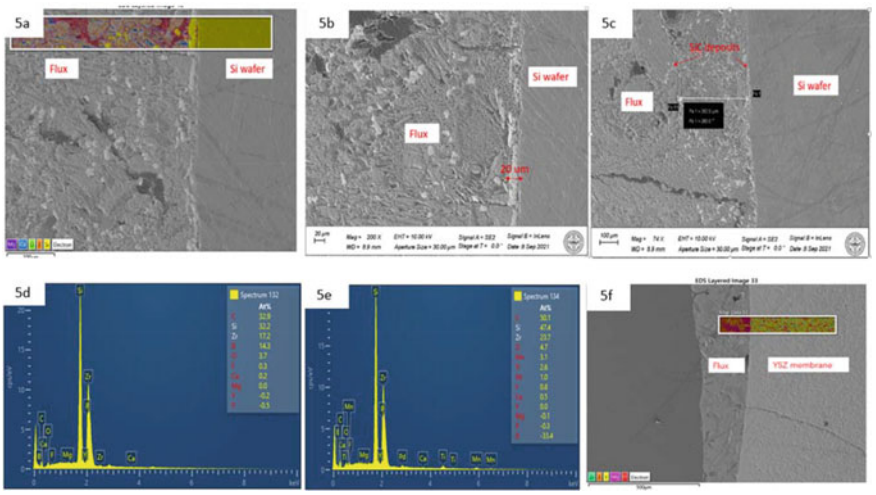

Fig. 5 SEM/EDS analysis of sectioned Si wafer and YSZ membrane **a** EDS mapping of the Si/Flux interface, **b** 20 μm thick SiC deposit on the Si wafer cathode, **c** dispersed SiC deposits in the flux adjacent to the Si wafer cathode, **d** EDX spectrum of the planar deposit close to Si wafer, **e** EDX spectrum of deposits dispersed in the flux adjacent to the Si wafer, **f** sectioned YSZ membrane in contact with flux along with EDS mapping post-electrolysis

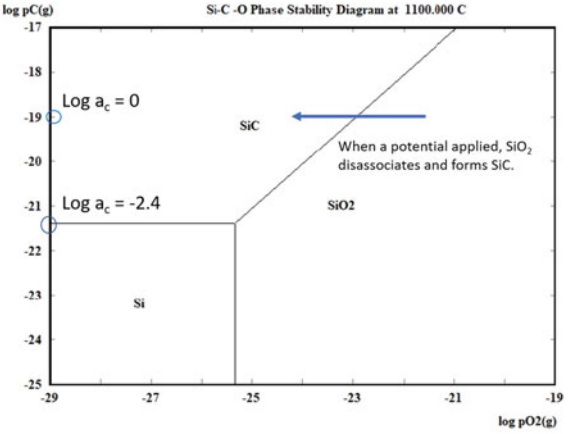

Fig. 6 Si-C-O phase stability diagram at 1100 C

electrolysis current. Some silicon carbide was also observed to be dispersed 450 μm in the flux adjacent to the silicon wafer (Fig. 5c). Further EDS point analysis on these two types of deposits indicates that they are mainly silicon carbide (Fig. 5d, e), with trace amounts of boron and phosphorous. Energy peaks of zirconium and phosphorous have strong overlap. The sources of boron and phosphorous are unclear. Furthermore, the section of the YSZ membrane in contact with the flux shows no diffusion of zirconium or yttrium into the flux (Fig. 5f). Thus, the YSZ membrane was stable in contact with the flux during the electrolysis. Therefore, it is unclear whether the observed Zr peak is real.

As previously discussed, silica dissociation occurred when the potential was greater than 0.51 V. It is likely that silicon was initially produced during the SOM electrolysis, but it reacted with carbon to form silicon carbide (The standard Nernst potential for reaction $SiO_2 + 3C = SiC + 3CO(g)$ at 1100 C is 0.32 V). This can also be explained from the phase stability diagram of Si-C-O (Fig. 6). In the presence of graphite (carbon at unit activity) when the applied potential is increased the oxygen activity decreases below 10^{-23} atm. and silica is reduced to SiC since Si is thermodynamically not stable. In order to reduce silica to Si the activity of carbon needs to be lower than $10^{-2.4}$.

Conclusions and Future Work

A state-of-the-art Solid Oxide Membrane Electrolytic Cell has been designed and assembled. An electrochemical reaction involving silicon wafer, flux, graphite, and impurity oxygen in the gas phase was shown to be responsible for the thinning of the wafer. By immersing the silicon wafer and the graphite current collector deep into the flux, this side reaction was significantly reduced. Subsequently SOM electrolysis of

silica with graphite as the current collector was performed. The process was electrochemically characterized, and the deposit was microstructurally and compositionally characterized. The SOM cell has an overall low resistance, and the salt electrolyte remained primarily ionic during electrolysis. It was found that silicon was successfully produced, but it formed a carbide phase due to the presence of graphite in the system (crucible and the current collector). YSZ membrane was found to be stable in contact with the flux during electrolysis.

Future work will focus in four priority areas. The first will be to remove all carbon components from the system. That includes the crucible and the current collectors. The carbon crucible will be replaced by a stainless-steel crucible. The carbon cathode current collector will be replaced by refractory tungsten metal and the carbon anode current collector will be replaced by an inert oxygen current collector developed earlier in our group [17, 18]. With these modifications we hope to be able to deposit pure silicon on the silicon wafer cathode and produce pure oxygen at the anode. Next, we will perform fluid-dynamics simulation to identify ways to lower concentration or mass transfer polarization to sustain the electrolytic current and increase the thickness of the silicon deposit. To lower surface roughness of the silicon deposit, we also plan to perform periodic current reversal with auxiliary electrodes in the salt flux, like that practiced in the copper industry. Finally, for longer-term operation we plan to replace liquid silver anodes, which volatilize, with stable lanthanum nickelates.

Acknowledgements This work was supported, in part, by the US Department of Energy's Office of Energy Efficiency and Renewable Energy (EERE) under the Solar Energy Technologies Office Award No. DE-EE0008988 and by the US National Science Foundation under Award Nos. CMMI-1937829 and 1937818.

References

1. Bye G, Ceccaroli B (2014) Solar grade silicon: technology status and industrial trends. Sol Energy Mater Sol Cells 130:634–646
2. Goodrich A et al (2013) A wafer-based monocrystalline silicon photovoltaics road map: utilizing known technology improvement opportunities for further reductions in manufacturing costs. Sol Energy Mater Sol Cells 114:110–135
3. Krishnan A, Lu XG, Pal UB (2005) Solid Oxide Membrane (SOM) technology for environmentally sound production of tantalum metal and alloys from their oxide sources. Scand J Metall 34(5):293–301
4. Suput M, DeLucas R, Pati S, Ye G, Pal U, Powell AC (2008) Solid oxide membrane technology for environmentally sound production of titanium. Trans Section C, Mineral Process Extract Metall 117(2):118–122
5. Pal UB (2008) A lower carbon foot print process for electrolytic production of metals from oxides dissolved in molten salts. JOM 60(2):43–47
6. Guan X, Pal UB, Powell AC (2014) Energy-efficient and environmentally friendly solid oxide membrane electrolysis process for magnesium oxide reduction: experiment and modeling. Metallurg Mater Trans E, Mater Energy Syst 1(2):132–144
7. Su S, Pal U, Guan X (2017) Solid oxide membrane electrolysis process for aluminum production: experiment and modeling. J Electrochem Soc 164(4):F248–F255

8. Jiang Y, Xu J, Guan X, Pal UB, Basu SN (2013) Production of silicon by solid oxide membrane-based electrolysis process. Mater Res Soc Symp Proceed 1493:231–235
9. Villalon T Jr (2018) Zero-direct emission silicon production via solid oxide membrane electrolysis. Doctoral dissertation, Boston University. https://hdl.handle.net/2144/30729
10. Xu J, Lo B, Jiang Y, Pal U, Basu S (2014) Stability of yttria stabilized zirconia in molten oxy-fluorite flux for the production of silicon with the solid oxide membrane process. J Eur Ceram Soc 34(15):3887–3896
11. Lovering DG, Gale RJ (eds) (1987) Molten salt techniques, vol 3. Plenum Press, New York, NY
12. Prasad S (2000) Studies on the Hall-Heroult aluminum electrowinning process. J Braz Chem Soc 11(3):245–251
13. Su S (2016) Zero-direct-carbon-emission aluminum production by solid oxide membrane-based electrolysis process. Doctoral dissertation, Boston University. https://hdl.handle.net/2144/17080
14. Krishnan A (2006) Solid oxide membrane process for the direct reduction of magnesium from magnesium oxide. Doctoral dissertation, Boston University (2006)
15. Gratz E, Pati S, Milshtein J, Powell AC, Pal UB (2012) Control of Yttrium diffusion out of yttria stabilized zirconia during SOM electrolysis for magnesium production. Magnes Technol:499–503, Sept
16. Virkar AV (2005) Theoretical analysis of the role of interfaces in transport through oxygen ion and electron conducting membranes. J Power Sources 147(1–2):8–31
17. Guan X, Pal UB, Gopalan S, Powell AC (2013) LSM (La0.8Sr0.2MnO3)-Inconel inert anode current collector for solid oxide Membrane (SOM) Electrolysis. J Electrochem Soc 160(11): F1179–F1186, Sep
18. Guan X, Pal UB, Jiang Y, Su S (2016) Clean metals production by solid oxide membrane electrolysis process. J Sustain Metall:152–166, Feb